CHEMICAL ENGINEERING TRANSACTIONS
VOL. 65, 2018
A publication of AIDIC
The Italian Association of Chemical Engineering
Online at www.aidic.it/cet
Guest Editors: Eliseo Ranzi, Mario Costa

ISBN978-88-95608- 62-4; **ISSN** 2283-9216
DOI: 10.3303/CET1865024

Ni/TiO_2 Catalysts for Liquid-Phase Hydrogenation of Levulinic Acid to γ-Valerolactone

Carlos Lanziano[a,b], Mayra M. Costa[a,b], Silvia F. Moya[b], Dean H. Barrett[b], Cristiane Rodella[b], Reginaldo Guirardello*[a]

[a] UNICAMP, School of Chemical Engineering, Av. Albert Einstein, 500, CEP 13083-852, Campinas, SP, Brasil
[b] Brazilian Synchrotron Light Laboratory (LNLS), Brazilian Center for Research in Energy and Materials (CNPEM), Zip Code 13083-970, Campinas, Sao Paulo, Brazil
guira@feq.unicamp.br

γ-Valerolactone (GVL) is a valuable and targeted biomass derivate used as a precursor in the production of liquid fuels and polymeric materials. It also finds application as a green solvent. However, the economic viability of GVL is dependent on its production cost from biomass, which relies heavily on the price and efficiency of the catalyst used in the hydrogenation process during levulinic acid (LA) conversion to GVL. Herein we show a catalyst with potential industrial applications for the conversion of LA to GVL. The catalyst is comprised of 35 wt.% Ni deposited onto TiO_2. Characterization was undertaken by XRD, N_2 physisorption and TPR analysis. The crystalline structure, surface area and porosity of the catalyst are similar to the TiO_2 support showing catalyst stability during and after activation. TPR analysis showed that Ni is reduced around 350 °C. The catalytic reaction was performed in a batch reactor under mild conditions (aq), 175 °C, 450 Psi H_2 whereby the catalyst was able to convert ≈ 80 % of LA, producing 76 % GVL. The reaction kinetics are presented and based on the Langmuir-Hinshelwood-Hougen-Watson (LHHW) rate equation.

1. Introduction

The production of fuels and chemicals from sustainable and renewable sources is a significant challenge facing mankind currently and will continue to face over the coming decades. Residual lignocellulosic biomass is one of the primary resources used to produce renewable fuels and chemicals. Lignocellulosic biomass is primarily composed of carbohydrate polymers (40 - 45 % cellulose and 25 - 30 % hemicellulose) and aromatic polymers (20 - 25 % of lignin) (Tang et. al. 2014). Various platform molecules/chemicals may be derived from these biomass carbohydrates, such as levulinic acid (LA) as shown in Figure 1 (Mukherjee et. al. 2015). In a successive step, LA can be converted to γ-valerolactone (GVL) via a catalytic hydrogenation route using supported noble metals (Ru, Pd and Ir) as catalysts in aqueous media under relatively mild conditions.
GVL is a value-added chemical and is currently used as a liquid fuel, food additive and solvent (Tang et. al. 2014). However, the high cost of noble metal catalysts is a prohibiting factor for industrial scale production using noble metal based catalysts (Wright and Palkovits 2012). Heterogeneous catalysts and external molecular H_2 sources are preferred due to ease of separation and catalyst recovery. More recently, supported non-noble metal catalysts have been investigated for LA conversion to GVL such as Ni, Cu, Fe, Cr supported on C, SiO_2, Al_2O_3 (Galletti et. al. 2012) as well as TiO_2 (Ruppert et. al 2015). In comparison to a highly efficient Ru/C catalyst (≥ 90 % conversion) using mild reaction conditions (130 °C, 174 Psi H_2 and 2h) (Yan et. al. 2009), non-noble catalysts currently produce low (≤ 15 %) to moderate (≤ 20 - 30 %) conversion under similar conditions. However, in some cases, these reactions make use of non-green solvents. A catalyst based on 20 wt.% Ni/TiO_2 showed promising results with ≈ 100 % conversion and ≈ 90 % selectivity to GVL in vapour phase hydrogenation reactions of LA. However, to attain these conversions high reaction temperatures (270 °C) are required as well as the reaction being performed in the vapour phase (Kumar et. al. 2015). Further studies are required to develop and investigate active and selective catalysts to economically produce GVL from LA. With the aim of exploring this subject, we developed a Ni/TiO_2 catalyst for aqueous phase hydrogenation of LA to GVL.

Please cite this article as: Lanziano C., Costa M., Moya S., Barrett D., Rodella C., Guirardello R., 2018, Ni/tio2 catalysts for liquid-phase hydrogenation of levulinic acid to γ-valerolactone, Chemical Engineering Transactions, 65, 139-144 DOI: 10.3303/CET1865024

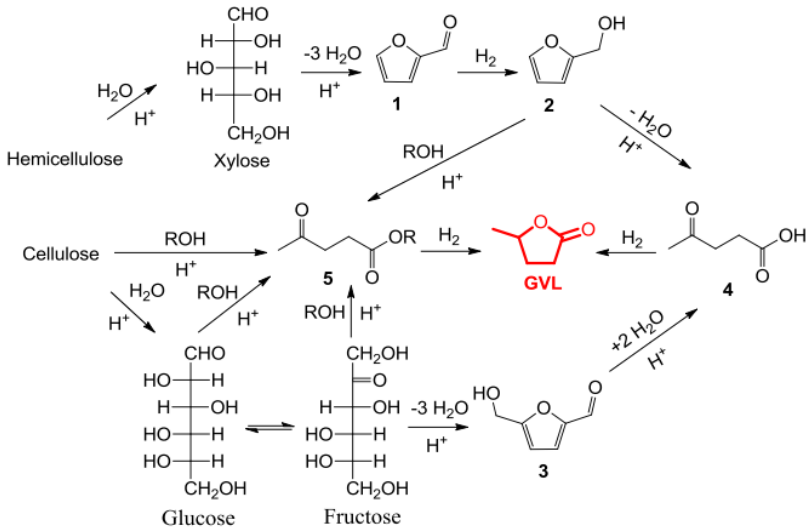

Figure 1. Reaction pathways leading to GVL from cellulose and hemicellulose: 1) furfural; 2) furfuryl alcohol; 3) HMF; 4) LA and 5) alkyl levulinates. Adapted from Mukherjee et. al. (2015).

2. Experimental

2.1 Catalyst Synthesis

Firstly, anatase phase TiO_2 was synthetized via sol-gel method consisting of the addition of 12 mL of titanium isopropoxide (Aldrich) added to 12.0 mL of 2-propanol (Merck) under stirring followed by the addition of 6.0 mL of water. Stirring was maintained for 1 h. The resulting solution was aged for 24 h. The product was then dried at 80 °C for 6 h and calcined at 450 °C for 16 h. Ni was then deposited on the resulting support with a theoretical loading of 35 wt.% using the deposition-precipitation method via NH_3 evaporation. 1.8 g of ammonium carbonate was added to a solution containing 20.0 mL of water and 20.0 mL of ammonium hydroxide solution (30 %, Sigma), under stirring at ambient temperature. 0.9216 g of nickel carbonate (Sigma) and 1.0 g of the TiO_2 were then added to the solution and heated to 80°C for 3 h under nitrogen atmosphere. After cooling to room temperature, the solid phase was extracted via centrifugation and washed with water until the pH is approximately 7, followed by drying at 80 °C overnight. Prior to characterization or catalytic testing, Ni was reduced via a thermal treatment to 400 °C under a flow of H_2 (50 mL/min, 10 °C/min heating rate). After 5 h at 400 °C, the catalyst was cooled and passivated using 1% O_2/He (50 mL/min for 12 h).

2.2 Characterization

X-ray diffraction (XRD) patterns were obtained at the XPD beamline at the LNLS/CNPEM. A beamline energy of 8.0 keV was used with the XRD data collected using a linear detector (Mythen 1k). Identification of crystalline phases was obtained from ICSD files. The crystallite sizes for TiO_2 were estimated using the Scherrer equation. Nitrogen adsorption-desorption isotherms were measured at -196 °C using a Quantachrome Autosorb-1C automatic analyzer. Samples were degassed at 120 °C for 13 h before isotherms were measured. The specific surface area values were determined using the BET model. The total pore volume was derived from the amount of gas absorbed at a relative pressure of P/P_0 = 0.95.

2.3 Catalytic Testing

Catalytic testing was performed using a Hastelloy batch reactor (300 mL, Parr Instruments). An aqueous solution of LA (35 g/L,Sigma) and 300 mg of catalyst were loaded into the reactor to give a total volume of 100 mL. The reactor was initially purged with N_2 followed by H_2 3 times. The initial pressure of hydrogen was 150, 300 and 450 Psi (at 30 °C). The reactor was heated to reaction temperature (175 °C) with a stirring speed of 50 rpm. The moment the reaction temperature was reached was considered the beginning of the reaction, the stirring speed was raised to 800 rpm and H_2 was added to the reactor. H_2 pressure was under isobaric conditions with pressures equal to 240, 475 or 710 Psi. At various points of the kinetic curve, samples from the reactor were taken for GVL and LA quantification.

2.4 Kinect Modeling

The kinetic models were developed considering the reaction between LA and H_2 to form 4-hydroxy pentanoic acid (HPA) °Ccurring over the surface of the catalyst with GVL formed homogenously in the liquid phase. The rate of transformation of LA and the formation of HPA and GVL are represented by Eq. (1) to (3).

$$r_{LA} = d\frac{[LA]}{dt} = -r_{surf}\frac{m_{cat}}{V} \quad (1)$$

$$r_{HPA} = d\frac{[HPA]}{dt} = r_{surf}\frac{m_{cat}}{V} - r_l \quad (2)$$

$$r_{GVL} = d\frac{[GVL]}{dt} = r_l \quad (3)$$

The reaction in the liquid phase is considered reversible and the rate is shown in Equation 4.

$$r_l = k_l\left([\mathrm{HPA}] - \frac{1}{K_l}[\mathrm{GVL}]\right) \quad (4)$$

The LHHW rate equation was used to model the reaction. Nine different models were obtained assuming the rate determining step is the adsorption of LA or H_2, the HPA desorption or the reaction over the surface. Additionally, considerations for the adsorption of H_2 over the catalyst are considered associative or non-dissociative. The models further consider that GVL is not reactive under the reaction conditions, but may however, adsorb over the metallic sites, hindering access to these active sites. The integration of the reaction rates and the modelling to the experimental data were programmed in python, using the scipy library (Jones E. et al., 2001). The models were integrated using an odeint scipy routine. The objective function, defined by the sum given in Eq (5), was minimized with the lmfit package (Newville et al. 2014). The value of the standard deviation was 5.1 and 1.0 mmol.L^{-1} for LA and GVL, respectively.

$$S = \sum_r \left[\frac{1}{\sigma_{gvl}^2}\sum_t \left(\hat{y}_{r,t}^{gvl} - y_{r,t}^{gvl}\right)^2 + \frac{1}{\sigma_{la}^2}\sum_t \left(\hat{y}_{r,t}^{la} - y_{r,t}^{la}\right)^2\right] \quad (5)$$

3. Results and Discussion

3.1 X-ray diffraction (XRD)

X-ray diffraction measurements were performed *in-situ* on the catalyst both before and after activation under a hydrogen containing, reducing atmosphere. The resulting diffractograms are shown in Figure 2.

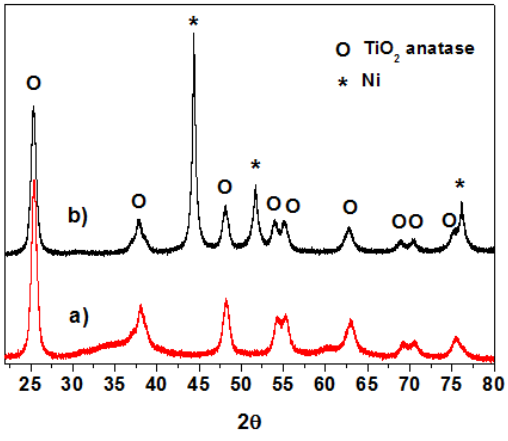

Figure 2. XRD patterns of 35 wt.% of Ni/TiO_2: a) as-prepared and b) after activation.

Diffractogram a) in Figure 2 shows the TiO_2 support consists of pure anatase phase with small crystallite sizes. The small amorphous background signal (2θ ≈ 30 – 38°) is attributed to the organic components of the starting precursors which have not been removed from the catalyst prior to activation. Once the activation of the catalyst takes place, the amorphous content of the catalyst is removed as seen in diffractogram b) of Figure 2. Further, the formation of a metallic Ni phase is also noted with reflections at 2θ ≈ 45 and 53°. The activation process showed no appreciable effect on the support material showing that the support remains stable throughout the activation process.

N_2 physisorption measurements of the pure TiO_2 and 35 %Ni supported on TiO_2 showed typical type IV adsorption isotherms (Fig. 3 left) related to mesoporous material which is confirmed by a large pore size distribution in the mesoporous region from 20 to 100 Å presented in Fig. 3 right (Chen et al. 2009). BET surface area value was 96 m^2/g for TiO_2 and 70 m^2/g for the 35% Ni/TiO_2 sample. The surface area reduction of the catalyst compared with the pure support is compatible with adding 35 wt.% of Ni onto the surface. Both adsorption-desorption isotherms and pore size distribution showed the catalyst maintain edits textural properties of the support with a small decrease in the gas volume adsorption and pore volume were detected due to Ni blocking the TiO_2 pores.

The reduction of nickel from Ni^{2+} to metallic Ni accounts for the observed TPR profile, as shown in Figure 4. Reduction began around 280 °C and continued as temperature was increased peaking around 350 °C. Based on this result, the regular procedure to activate the catalyst prior to catalytic reaction consists of heating to 400 °C for 5 h to ensure complete Ni reduction.

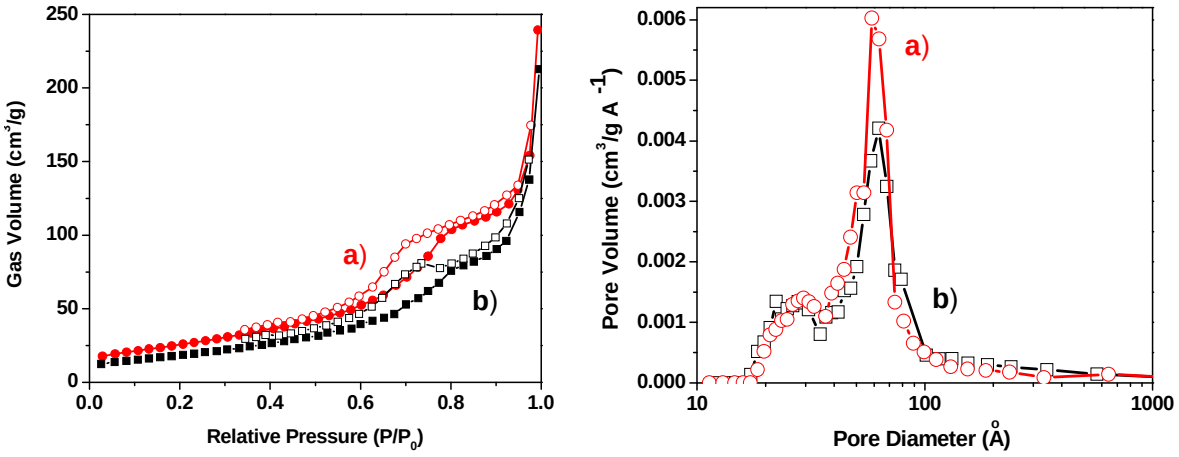

Figure 3. Adsorption-desorption isotherms (left) and pore size distribution curves (right) of samples: a) TiO_2 (support) and b) 35% Ni/TiO_2 after activation.

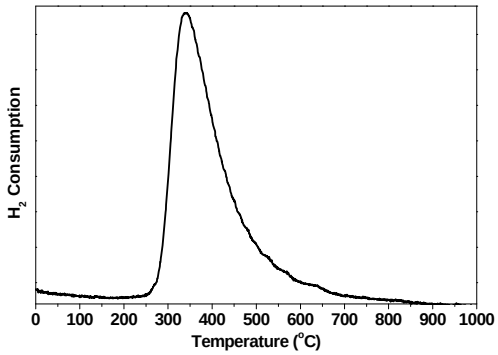

Figure 4. TPR profile of 35% Ni/TiO_2 during activation.

4. Catalytic testing

The conversion of LA and yield of GVL at various pressures are shown in Figure 5 (left and right) respectively. An increase in hydrogen pressure considerably affects the LA conversion rate. When 450 and 300 Psi H_2 pressure was used, conversion figures of 79 % and 72 % were achieved respectively. In comparison, only 47 % LA conversion was reached with 150 Psi H_2. Maximum respective GVL yields of 44 %, 63 % and 76 % were obtained when H_2 pressures were increased from 150 to 300 Psi, and finally to 450 Psi. Although GVL selectivity was high for all pressure values used in this work, the most noticeable increase was seen when 450 Psi was used compared to 300 Psi raising the GVL yield from 40 to 76 %. Maximum productivity was 0.03 mol (GVL) . g $(Ni)^{-1}$. h^{-1}, comparable with reported results for 48 % Ni/TiO_2 prepared by deposition-precipitation method (Jinkun et al. 2015) using isopropyl alcohol as solvent, and higher than the reported results for nickel catalysts using water as solvent (Shimizu et al. 2014; Gundekari and Srinivasan 2017).

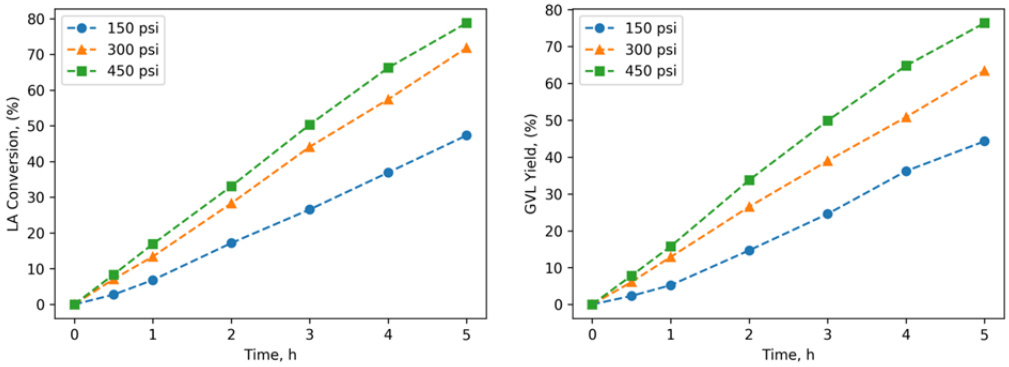

Figure 5. Catalytic activity of 35% Ni/TiO_2 catalyst for levulinic acid hydrogenation.

5. Modeling

The best fits were obtained using two models, A and B, from the nine models previously obtained. Both models consider that the rate determining step is that of the surface reaction. Model A is obtained with the assumption that H_2 adsorption is non-dissociative, while model B considers that H_2 adsorption is dissociative and the rate determining step is the hydrogenation of LA to an intermediate over the surface ($HLA \cdot l$). The initial fit of the data showed that the equilibrium adsorption of HPA and GVL are not significant. This implies that GVL formation does not impede the active sites of the catalyst. Therefore, the models were reduced to the form shown in Equations 6 and 7, for models A and B, respectively.

$$r_{surf} = k_{sr} K_{H_2} K_{LA} [LA][H_2] / \left(1 + K_{AL}[AL] + K_{H_2}[H_2]\right)^2 \quad (6)$$

$$r_{surf} = k_{sr_1} K_{H_2} K_{LA} [LA][H_2] / \left(1 + K_{AL}[AL] + \left(K_{H_2}[H_2]\right)^{1/2}\right)^2 \quad (7)$$

To discriminate between model A and B, an additional experimental data set was used (175 °C, 280 Psi and 20 g . L^{-1} LA). With the additional data model A produced the best fits. The value of S obtained was 246 and 363, for models A and B, respectively. Model A was therefore selected and the parameter values were recalculated using the new data. The values of the parameters are showed in the Table 1.

Table 1. Optimized parameters with 95 % confidence intervals using model A

Model A1 (considering k_l) S =544, S_{red} = 12.4					Model A2 (considering $k_l \gg 0$) S =685, S_{red} = 15.2		
Parameter	K_{H_2}	K_{LA}	k_{sr}	k_l	K_{H_2}	K_{LA}	k_{sr}
units	L/mol	L/mol	mol/g_{cat}·h	1/h	L/mol	L/mol	mol/g_{cat}·h
Best value	19.7	8.22	0.132	9.1	20.7	8.7	0.124
Lower*	16.1	7.51	0.125	7.1	16.5	7.2	0.112
upper*	24.3	8.99	0.138	22.2	26.0	9.6	0.133

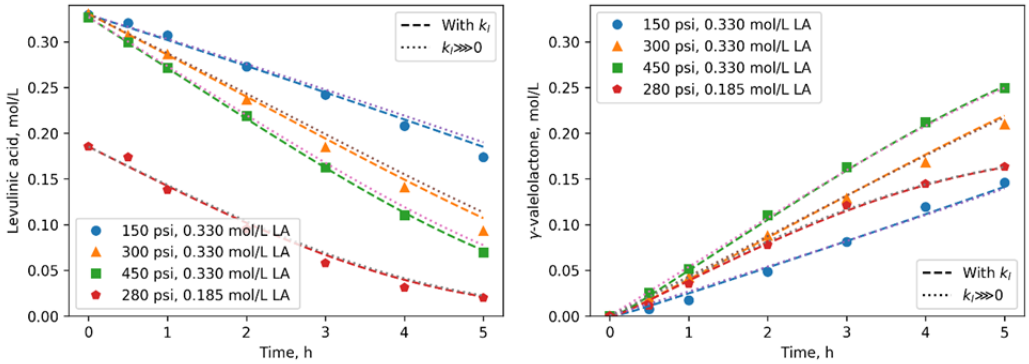

Figure 6. Experimental data and predicted data with model A, with k_l and without ($k_l \gg 0$).

Analyses of the confidence intervals show that parameter k_l has high uncertainty, primarily in its upper limit (Table 1). The parameter k_l is related to the HPA in solution. A high value of k_l implies the HPA is rapidly converted to γ-valerolactone (GVL) and therefore the concentration of HPA remains low. The converse is also true. As concentration of HPA is not measured directly the model infers its value from the concentration of LA and GVL. However, due to high GVL selectivity the HPA concentration gave higher uncertainty values comparable to those attained from LA. Due to the high uncertainty, the parameter was not considered and new parameter values are shown in the Table 1. Figure 6 compares the predicted values using model A with and without k_l ($k_l \gg 0$).

6. Conclusions

The synthesized Ni/TiO_2 catalyst efficiently catalyzes the hydrogenation of LA to GVL under mild reaction conditions, revealing a potential cost-effective catalyst for industrial application. Almost 80 % of LA was converted into GVL (76 % yield) at 175 °C, 450 Psi H_2, 5 h (aq). Structural and textural properties of the catalyst are similar to the TiO_2 support showing catalyst stability during activation and under operation. The results further demonstrated that the 35 wt.% Ni loading did adversely affect the catalysts activity due to a stable, mesoporous anatase (TiO_2) phase with high surface area (76 m^2/g). The LHHW method was used to interpret the experimental data and showed that the production of GVL does not poison the catalyst. Further studies are required to determine the link between the LA concentration and the reaction temperature and their effects on the rate constant for the overall reaction.

Acknowledgments

We would like to thank CAPES for C. A. S. Lanziano scholarship and LNLS/CNPEM for infrastructure and staff.

References

Chen, D., Huang, F., Cheng, Y.-B. and Caruso, R. A., 2009, Mesoporous Anatase TiO2 Beads with High Surface Areas and Controllable Pore Sizes: A Superior Candidate for High-Performance Dye-Sensitized Solar Cells, Adv. Mater. 21, 2206–2210. doi:10.1002/adma.200802603

Galletti, A. M. R., Antonetti, C., Luise, V. D., & Martinelli, M., 2012, A sustainable process for the production of γ-valerolactone by hydrogenation of biomass-derived levulinic acid, Green Chemistry 14, 688-694.

Gundekari, S.; Srinivasan, K., 2017, In situ generated Ni(0)@boehmite from NiAl-LDH: An efficient catalyst for selective hydrogenation of biomass derived levulinic acid to γ-valerolactone, Catalysis Communications 102, 40–43.

Jinkun, Lv., Rong, Z., Wang, W., Xiu, J., Wang, Y., and Qu, J., 2015, Highly efficient conversion of biomass-derived levulinic acid into γ-Valerolactone over Ni/MgO catalyst, RSC Adv. 5, 72037.

Jones E, Oliphant E, Peterson P, et al., 2001, SciPy: Open Source Scientific Tools for Python, <http://www.scipy.org>accessed 16.11.2017.

Kumar, V. V., Naresh, G., Sudhakar, M., Tardio, J., Bhargava, S. K., & Venugopal, A., 2015,. Role of Brønsted and Lewis acid sites on Ni/TiO 2 catalyst for vapour phase hydrogenation of levulinic acid: Kinetic and mechanistic study, Applied Catalysis A: General 505, 217-223.

Mukherjee, A., Dumont, M. J., & Raghavan, V., 2015, Sustainable production of hydroxymethylfurfural and levulinic acid: Challenges and opportunities, Biomass and Bioenergy 72, 143-183.

Newville, M., Stensitzki, T., Allen, D. B., & Ingargiola, A., 2014, LMFIT: Non-Linear Least-Square Minimization and Curve-Fitting for Python, Zenodo. DOI: 10.5281/zenodo.11813.

Ruppert, A. M., Grams, J., Jędrzejczyk, M., Matras-Michalska, J., Keller, N., Ostojska, K., & Sautet, P., 2015. Titania-Supported Catalysts for Levulinic Acid Hydrogenation: Influence of Support and its Impact on γ-Valerolactone Yield, ChemSusChem 8 (9), 1538-1547.

Shimizu, K.-I.; Kanno, S.; Kon, K., 2014, Hydrogenation of levulinic acid to γ-valerolactone by Ni and MoO co-loaded carbon catalysts, Green Chemistry 16, 3899-3903.

Tang, X., Zeng, X., Li, Z., Hu, L., Sun, Y., Liu, S., ... & Lin, L., 2014, Production of γ-valerolactone from lignocellulosic biomass for sustainable fuels and chemicals supply, Renewable and Sustainable Energy Reviews 40, 608-620.

Wright, W. R., & Palkovits, R., 2012, Development of heterogeneous catalysts for the conversion of levulinic acid to γ-valerolactone, ChemSusChem 5 (9), 1657-1667.

Yan, Z. P., Lin, L., & Liu, S., 2009, Synthesis of γ-valerolactone by hydrogenation of biomass-derived levulinic acid over Ru/C catalyst, Energy & Fuels 23 (8), 3853-3858.